Lessons learned from the QUENCH-LOCA experiments

J. Stuckert, M. Große, M. Steinbrück, M. Walter, A. Wensauer

Seven QUENCH-LOCA bundle tests (QUENCH-L0…-L5 and -L3HT) with different cladding materials (Zry-4, M5®, Opt. ZIRLO™) were performed according to a temperature/time-scenario typical for a LBLOCA in German PWRs. For two tests (QUENCH-L4 and -L5) pre-hydrogenated claddings (with 100 and 300 wppm H for M5® and Opt. ZIRLO™, correspondingly) were used. Generally, a peak cladding temperature of about 1350 K (1250 K for QUENCH-L5) was reached at the end of the heat-up phase at the bundle elevation of 950 mm. The maximal heat-up rate was 8 K/s (2.6 K/s for commissioning test QUENCH-L0); the cooling phase lasted about 120 s (0 s for QUENCH-L0) and was terminated by 3.3 g/s/effective rod water flooding. The tangential temperature gradient across a rod was between 30 and 70 K on the burst onset.

The detailed profilometry measurements performed over whole length of the claddings showed formation of not only main ballooning area (with burst) but also, for several rods of each bundle, additional two or three ballooning regions. Another parameter calculated based on profilometry measurements is the bundle blockage. The maximal coolant channel blockage was less than 35%. Due to the moderate blockage good bundle coolability was kept for all bundles.

Cladding wall thinning from 725 to 350 µm due to ballooning was observed at the burst side along 50 mm below and above burst opening. The maximal oxide thickness at the outer cladding surfaces was less than 15 µm. Surface cracks, penetrating both layers, were formed in vicinity of burst opening during ballooning. Oxide layer formed after the burst at the inner cladding surface around the burst opening with a thickness of about 15 µm decreasing to 3 µm at a distance of about 20 mm from the burst opening.

The hydrogen, produced during oxidation of the inner cladding surface around the burst opening, can be absorbed by the metal with formation of hydrogen enrichments around the oxidized area (secondary hydrogenation). Such enrichments with a quite complex 3D form were observed for inner rods having been exposed to peak cladding temperatures of more than 1200 K. Except for the QUENCH-L0 test, no hydrogen bands were observed for bundle outer rods, the peak cladding temperature measured for these rods was less than 1200 K. Neutron tomography analyses showed (except the QUENCH-L0 bundle with non-prototypical long duration of the transient stage and the QUENCH-L3HT with not prototypical high temperatures) that the maximal hydrogen concentrations inside the hydrogen bands was less than 750 wppm (averaged through the cladding cross section). EBSD analysis showed that a part of the hydrogen absorbed inside the claddings formed the hydrides with µm-sizes, which are distributed in the matrix intra as well inter granular. Another part of the absorbed hydrogen was probably dissolved in the metallic matrix.

During quenching, following the high-temperature test stages, no fragmentation of claddings was observed meaning that the residual strengths and ductility were sufficient.

Tensile tests at room temperature evidenced fracture at hydrogen bands for several inner rods with local hydrogen concentrations about 1500 wppm and more. Claddings with lower hydrogen concentrations fractured due to stress concentration at burst opening edges. Other tensile tested claddings failed after necking far away from burst region.

Lessons learned from the QUENCH-LOCA experiments

KIT: J. Stuckert, M. Große, M. Steinbrück, M. Walter,
VGB: A. Wensauer

QWS-23, Karlsruhe 2017

Institute for Applied Materials; Program NUKLEAR

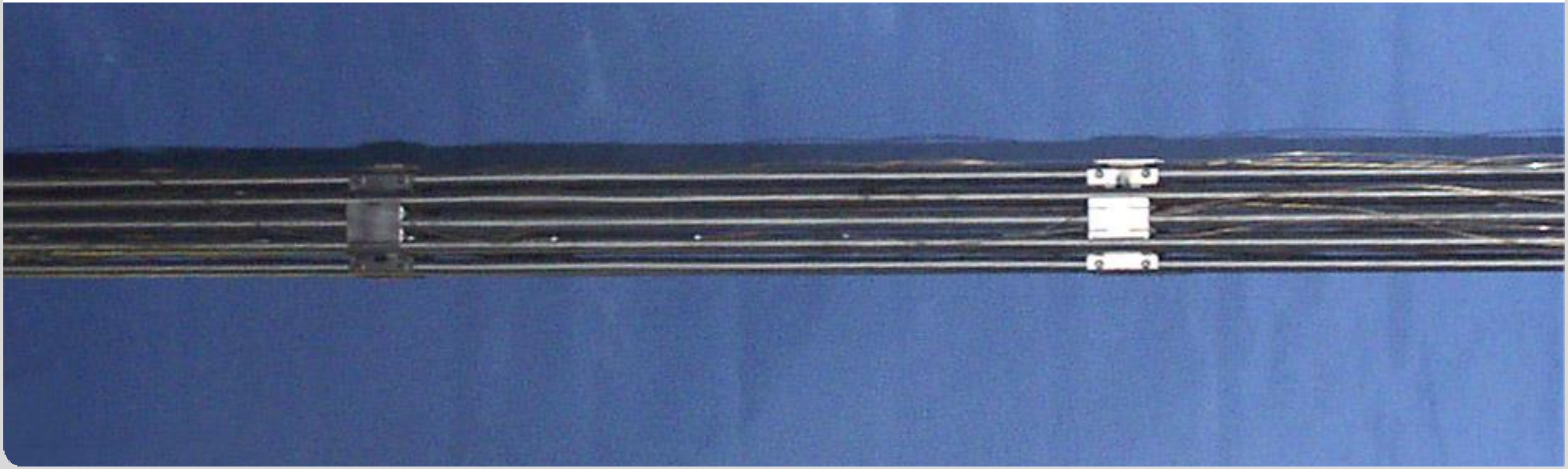

QUENCH-LOCA Test Matrix 2010 – 2016

Test	Type of cladding tubes	Max heat-up rate, K/s	Max T on the end of heat-up, K	Duration of inner clad. oxidation at T > 1123 K, s	Secondary cladding hydro-genation	Post-test fracture due to second. hydro-genation
Commissioning QUENCH-L0 July 22, 2010	Zry-4	2.5	1350	110	yes	yes
Reference QUENCH-L1 Feb. 02, 2012	Zry-4	7	1373	105	yes	no
QUENCH-L2 July 30, 2013	M5®	8	1373	88	yes	no
QUENCH-L3HT March 21, 2014	Opt. ZIRLO™	8	1623	252	yes	yes
QUENCH-L4 July 30, 2014	Pre-hydr. M5® (100 wppm H)	8	1385	100	yes	yes
QUENCH-L3 March 17, 2015	Opt. ZIRLO™	8	1346	84	yes	no
QUENCH-L5 Feb. 17, 2016	Pre-hydr. opt. ZIRLO™ (300 wppm H)	8	1257	45	no	-

Hardware elements

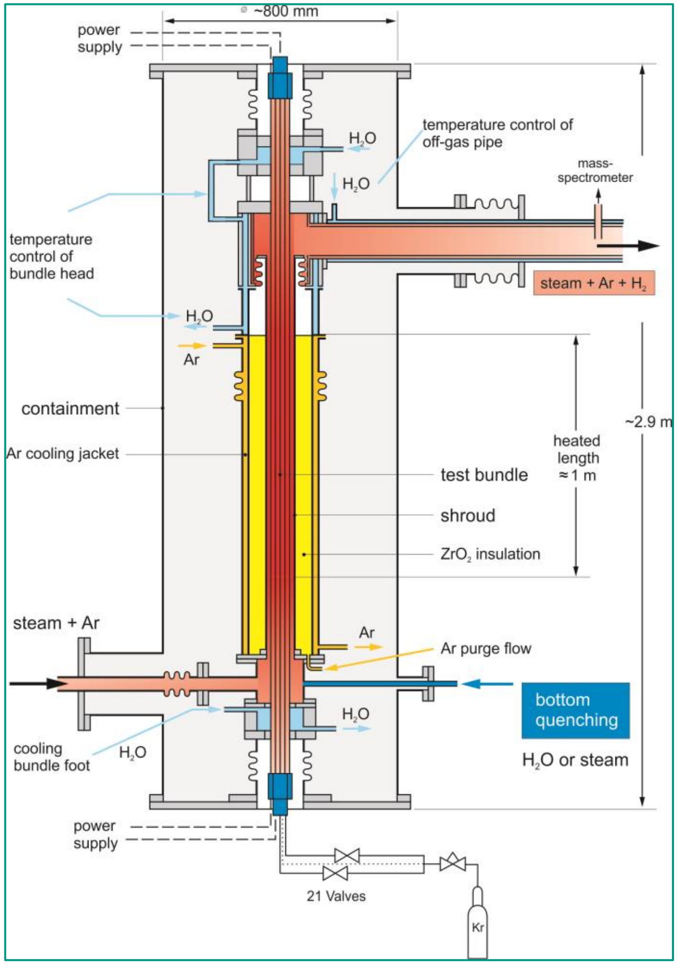

QUENCH facility:

test section with flow lines

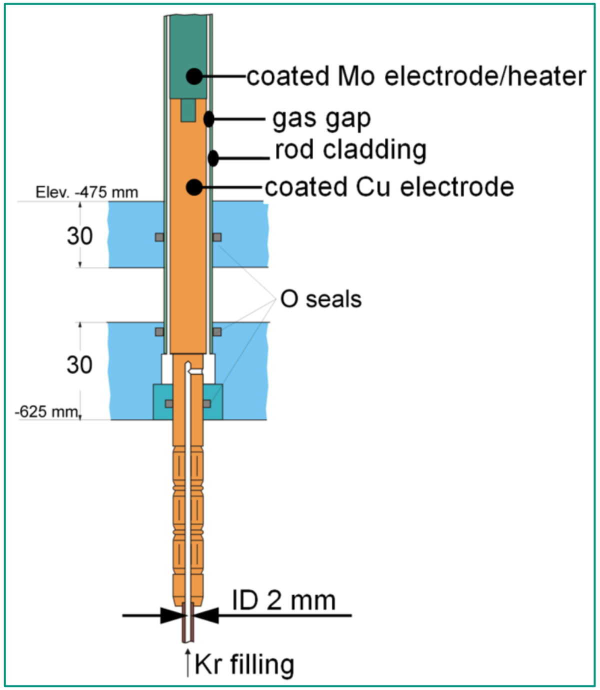

Rod pressurization from bottom of each rod

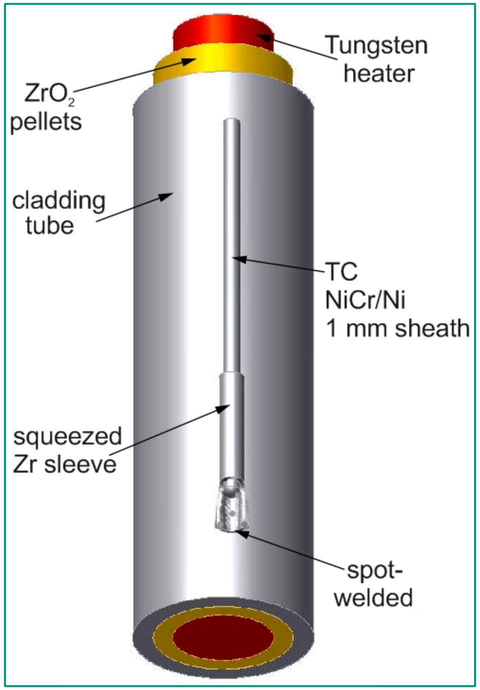

TC fastening at the test rod

Cross-sections of the QUENCH-L2 … -L5 bundles

QL-2, QL-4

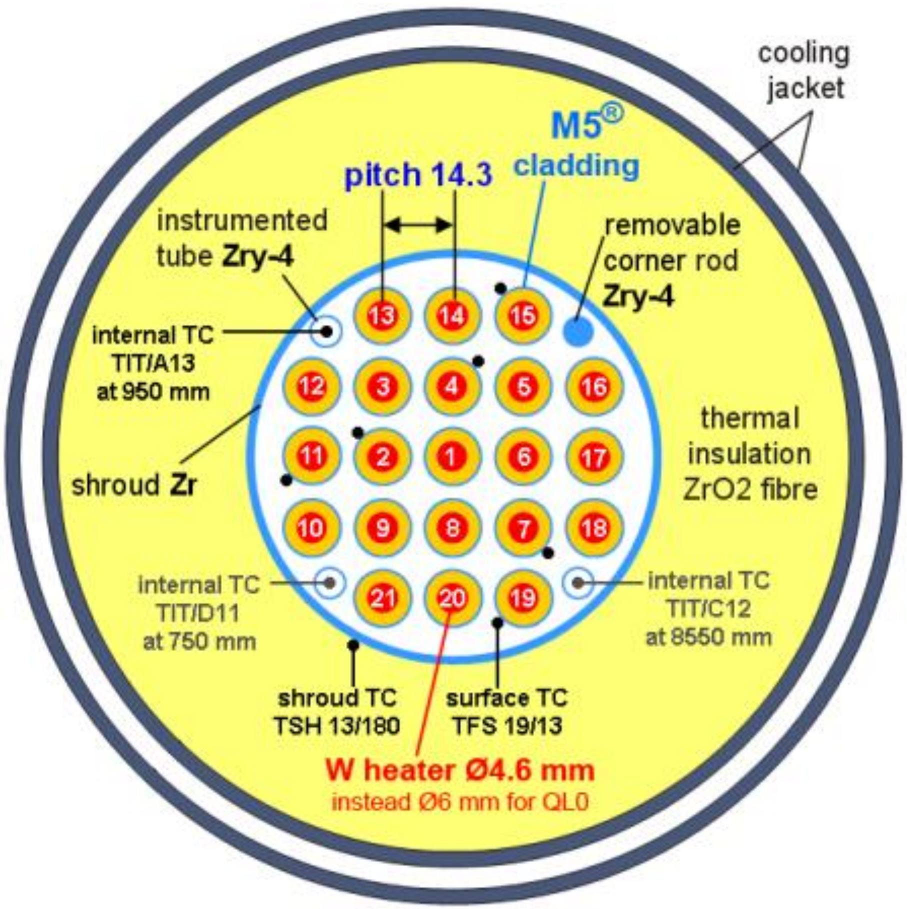

QL-3, QL-3HT, QL-5

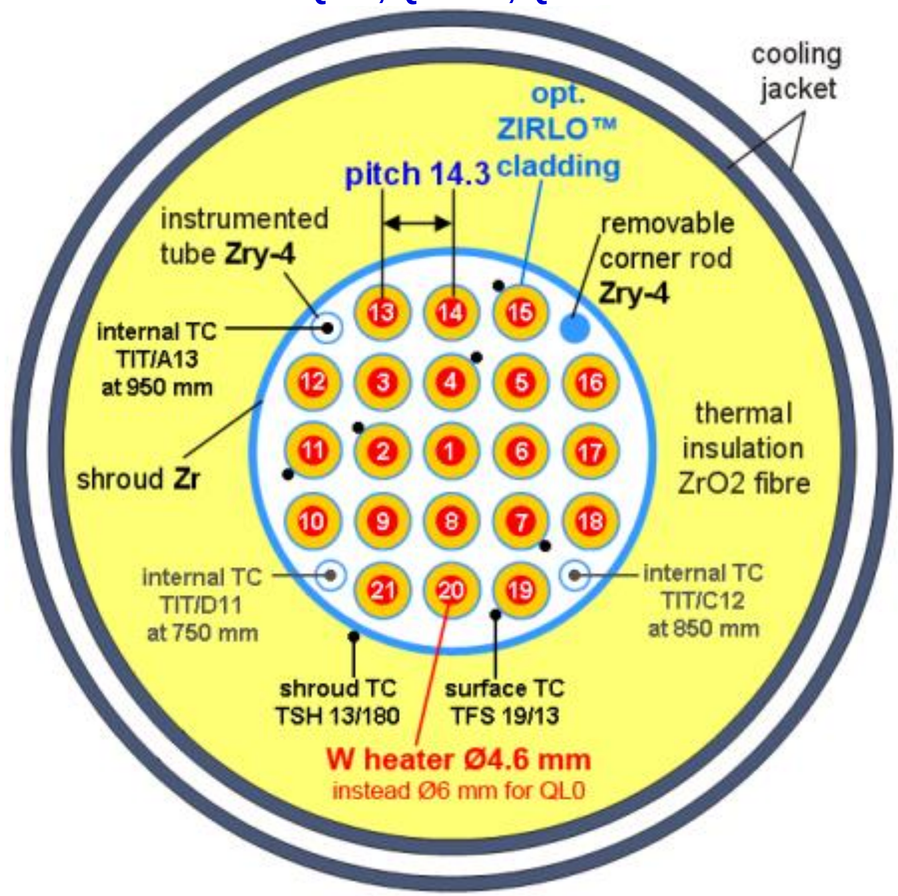

1) The use of ***tungsten*** heaters with smaller diameter (***4.6 mm***) instead tungsten heaters (QUENCH-L0) or tantalum heaters (QUENCH-L1) with diameter of 6 mm has allowed to reach a **higher heat rate**.
2) All rods are filled with Kr with p=55 bar at T_{pct}=800 K (similar to QUENCH-L1).

Test progresses

M5: QL-2, QL-4

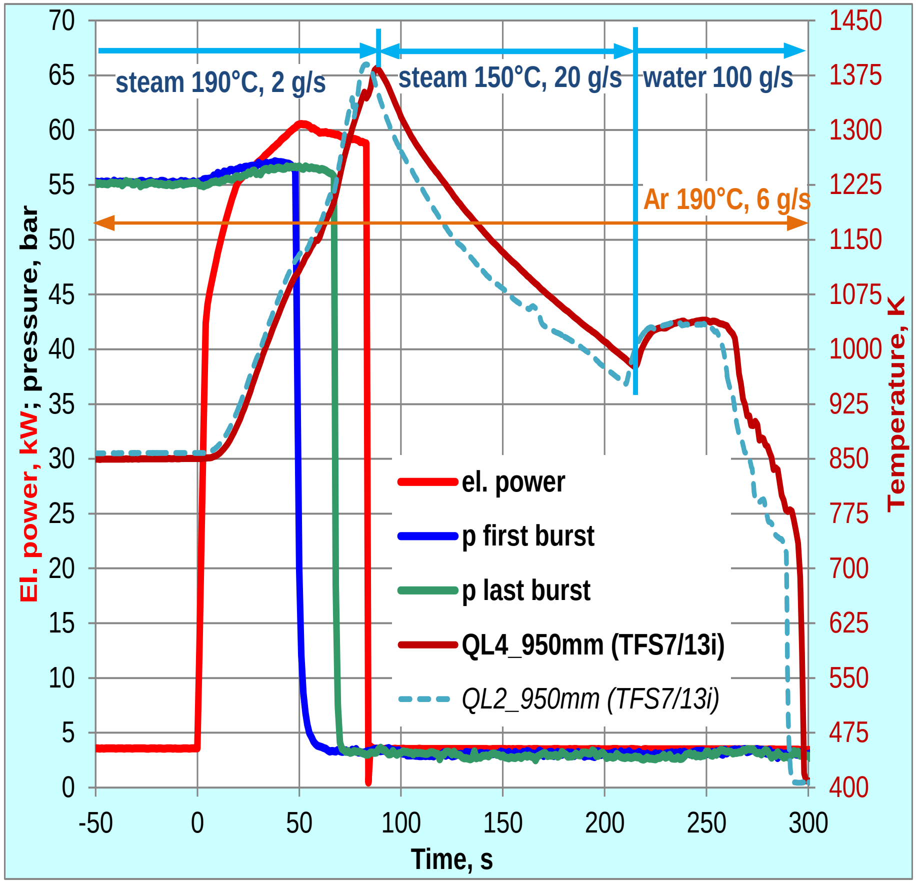

Opt. ZIRLO: QL-3, QL-5

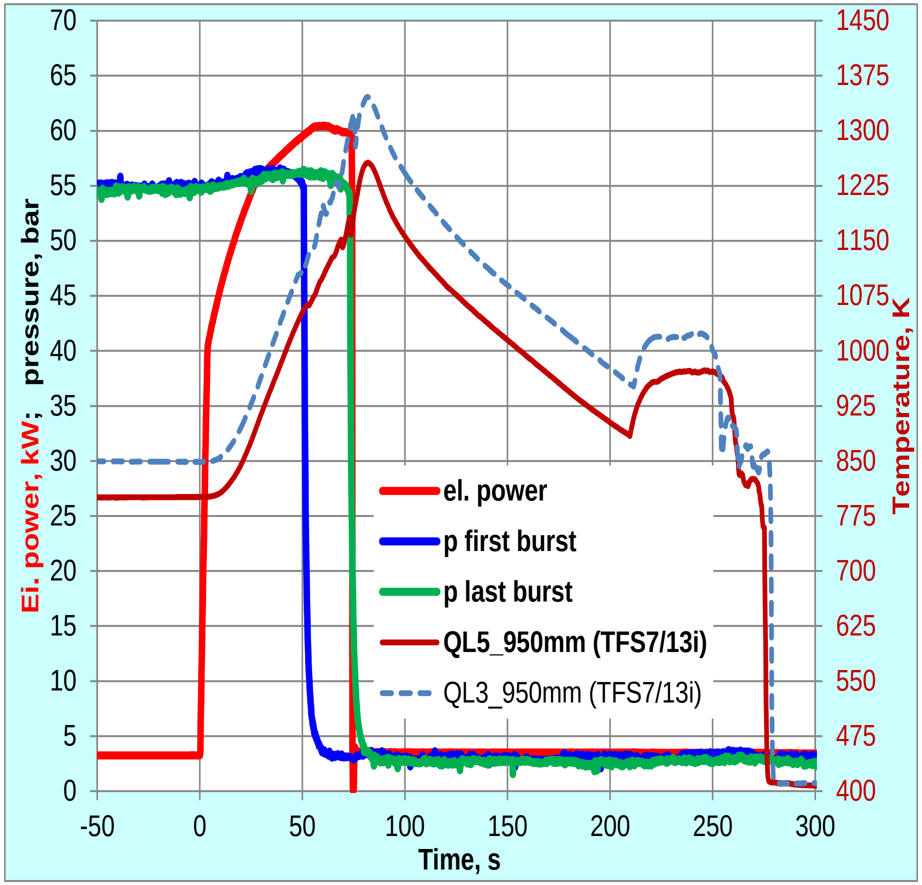

Dependence of radial temperature difference (for rod #7 of QL3 and QL5 bundles)

from position of contact between pellet and cladding

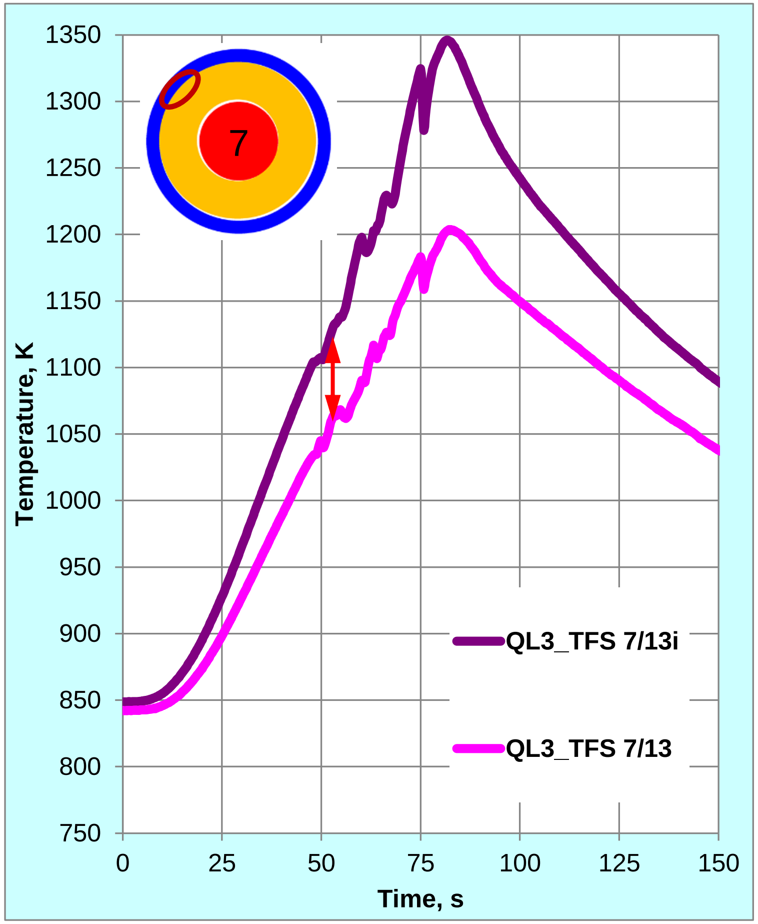

QL-3

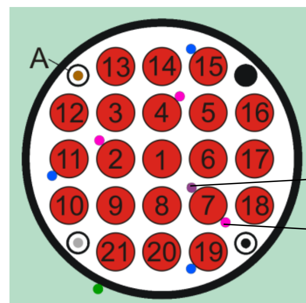

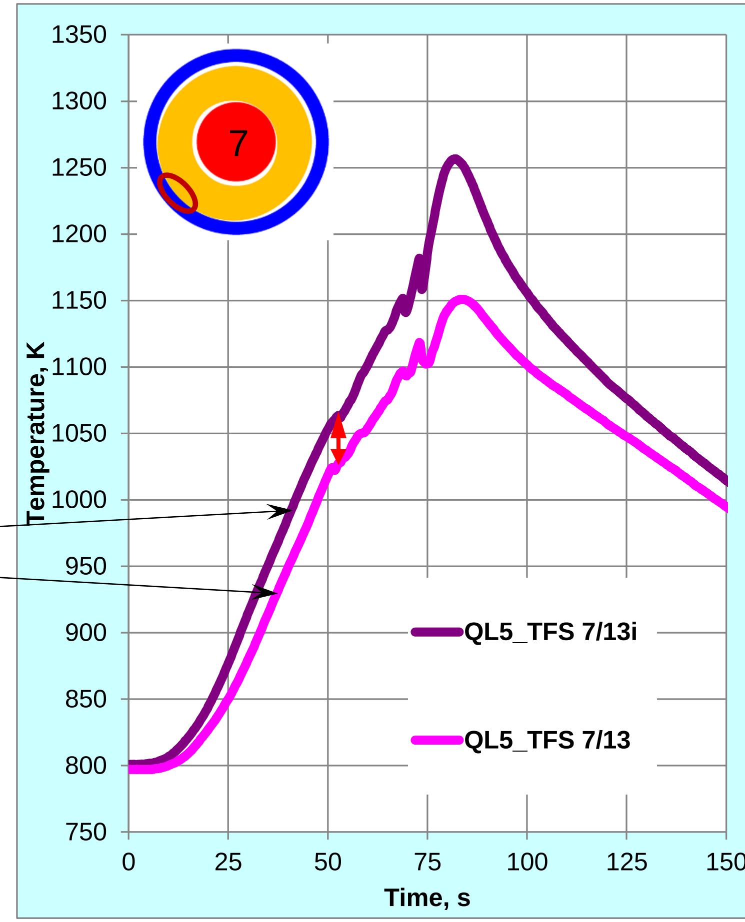

QL-5

Superposition of two temperatures gradients:
global bundle gradient (from shroud to central rod) and local gradient inside rod

Axial temperature profiles on first cladding burst

and end of transient

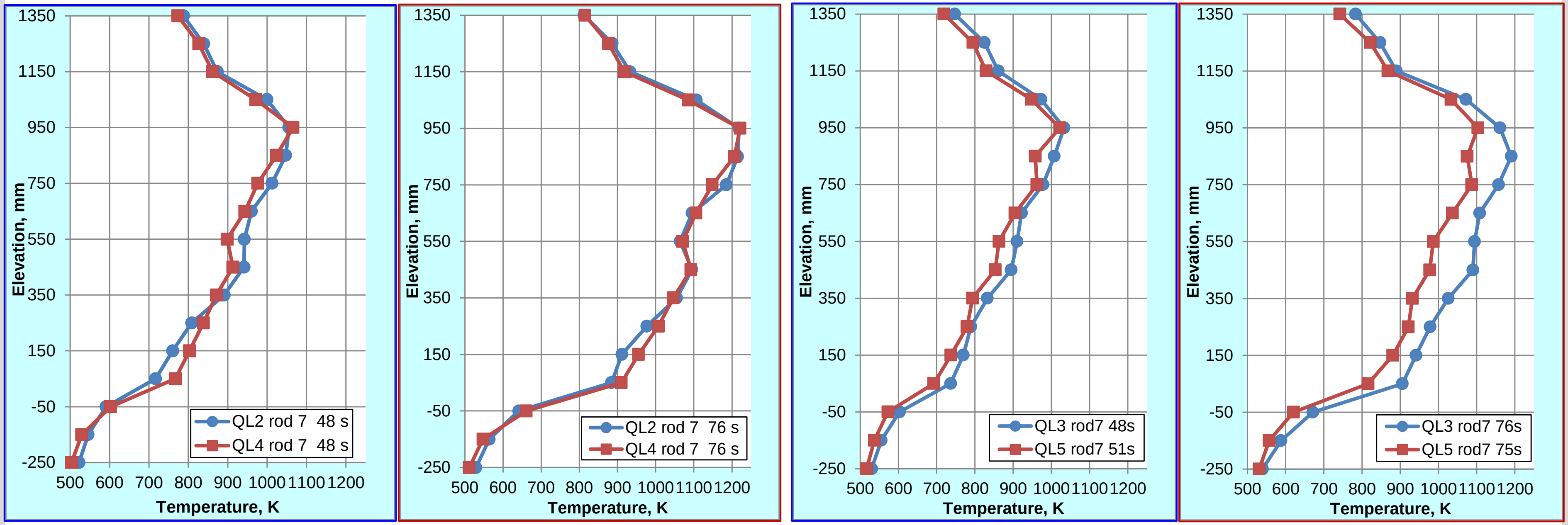

QL-2 and QL-4

QL-3 and QL-5

Off-gas mass spectrometer measurements: steam and H_2

steam release (25 g/s)
during reflood (100 g/s water)

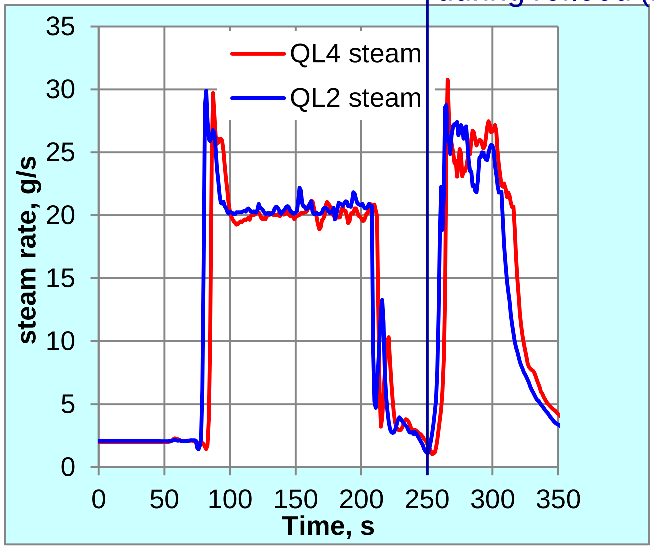

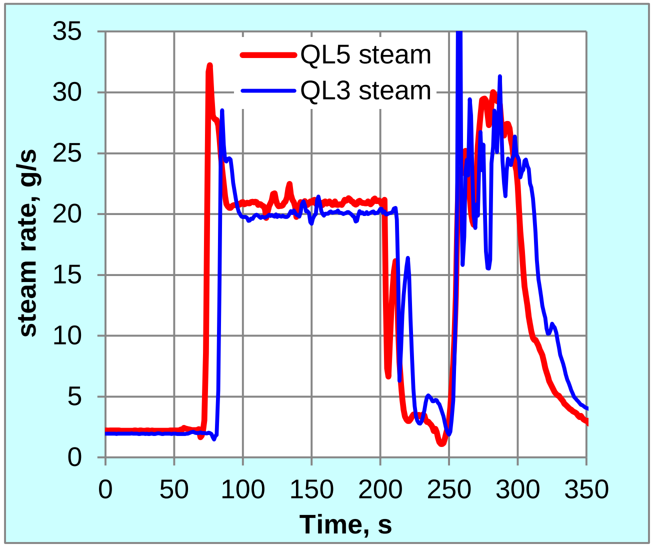

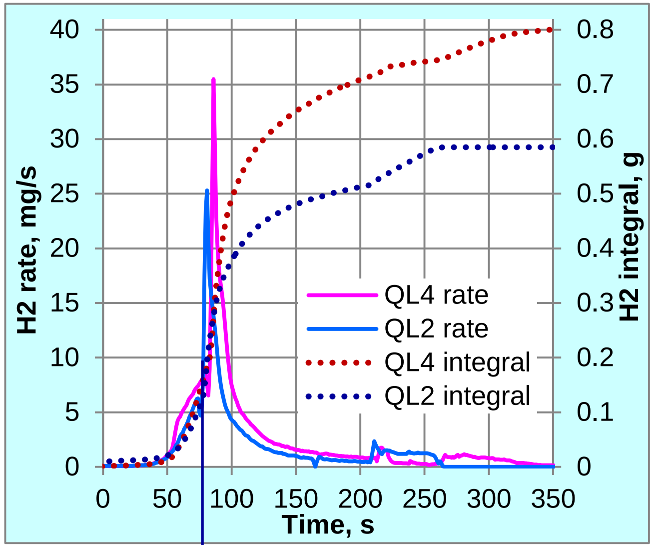

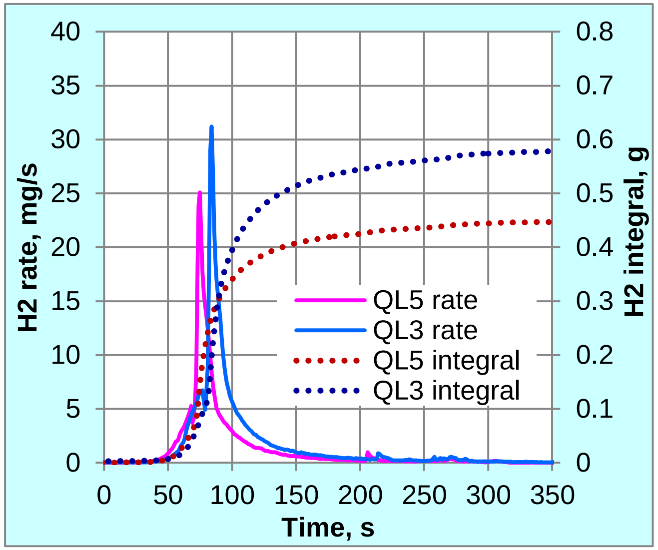

H_2 increase during heat-up

H_2 peak at initiation of cool-down in 20 g/s steam

Post-test views of different bundles in the burst region

QL-1, view at 180°

QL-2, view at 270°

QL4, typical view for all QL-3, -4, -5 bundle positions

Increased bending of QL-0, QL-1, QL-2 and QL-3HT rods due to limited axial heater expansion

Videoscope observations with camera inserted from the bundle bottom at positions of corner rods

Karlsruhe Institute of Technology

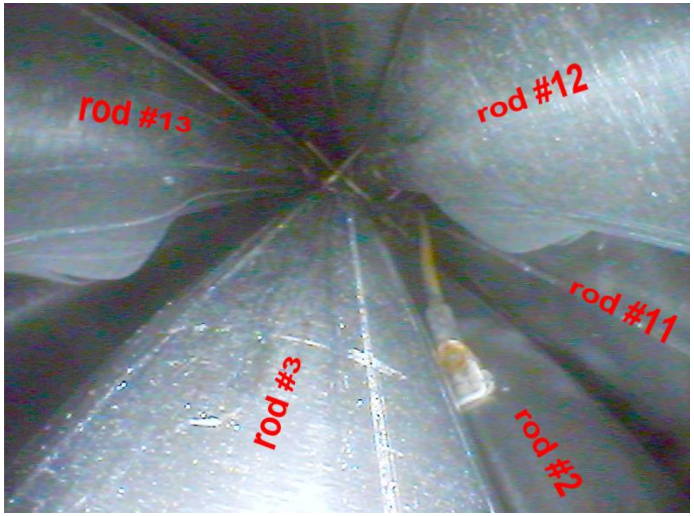

QL-2, at corner rod A

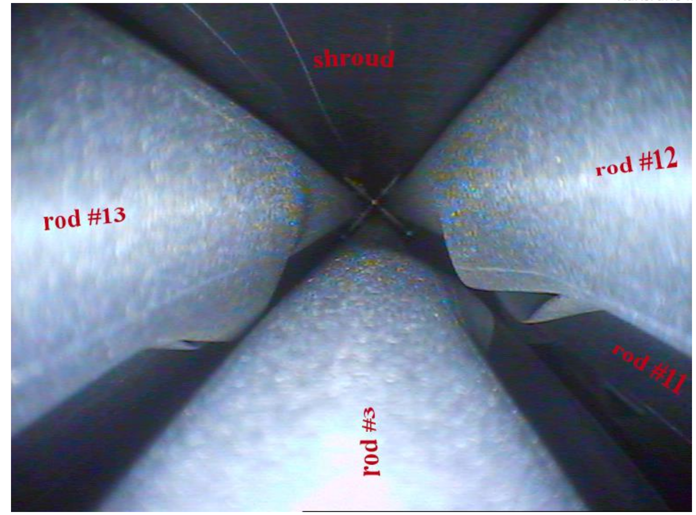

QL-3, at corner rod A

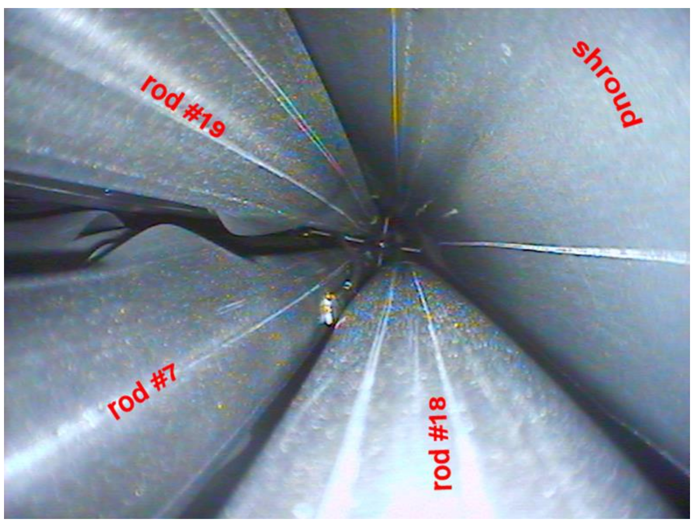

QL-4, at corner rod C

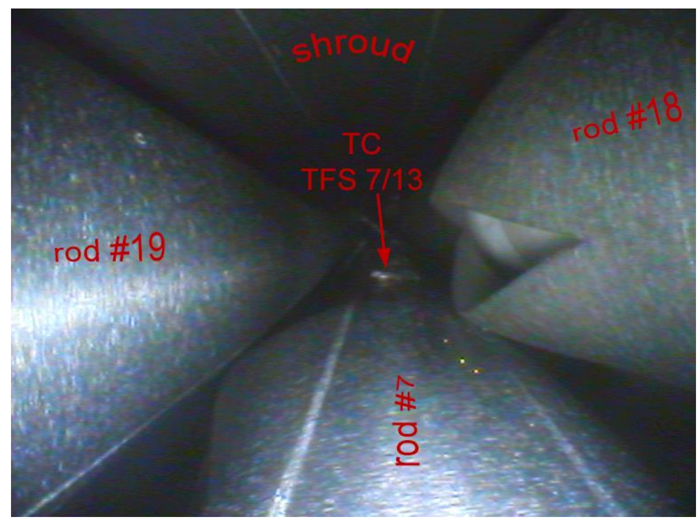

QL-5, at corner rod C

Radial and axial positions of burst openings

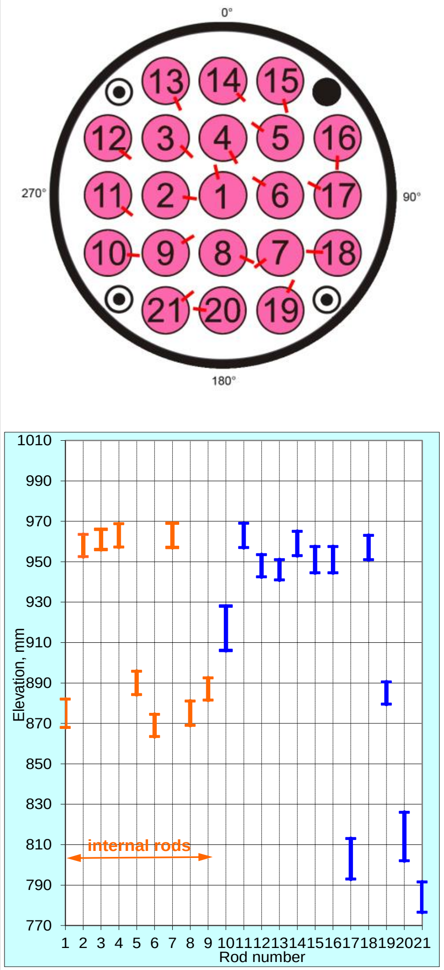

QL-2 (M5®)

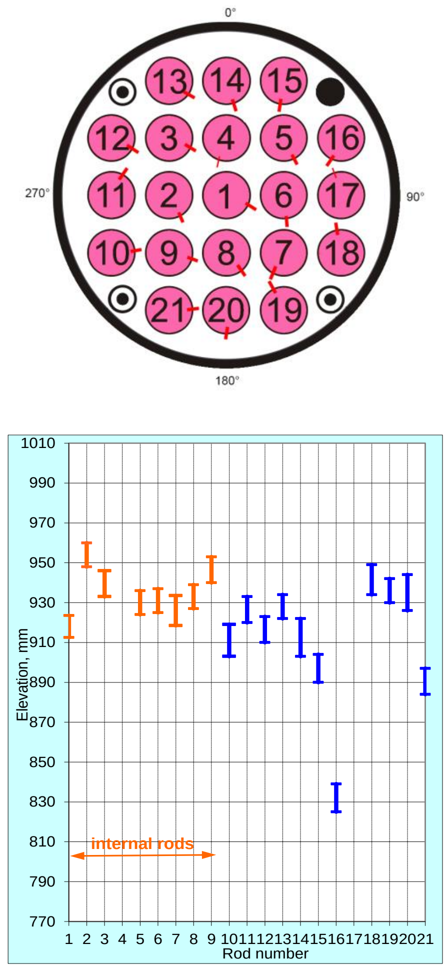

QL-4 (hydrogenated M5®)

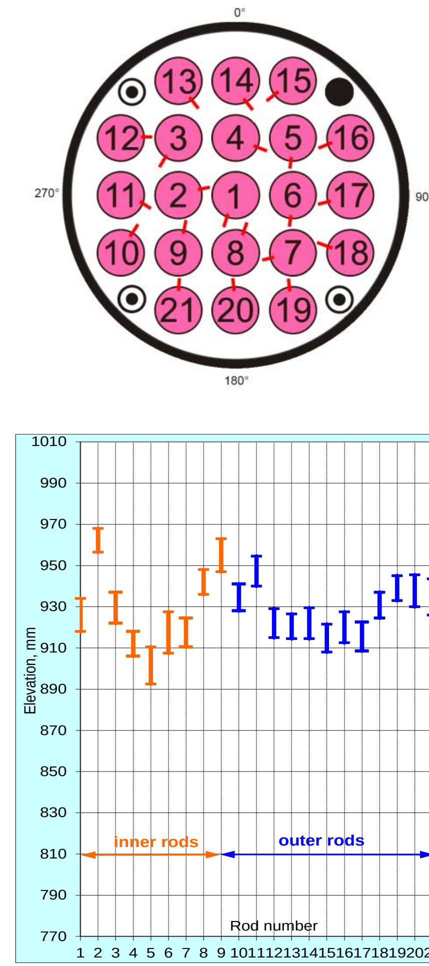

QL-3 (opt. ZIRLO)

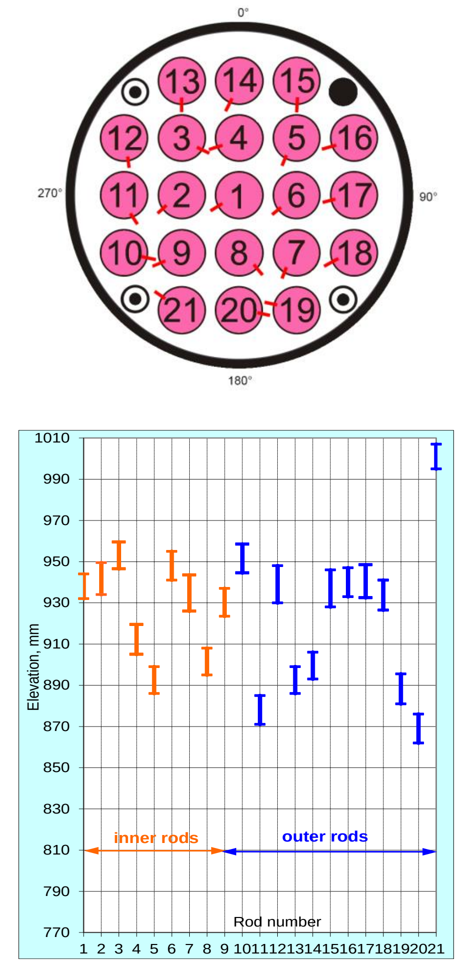

QL-5 (hydrogenated opt. ZIRLO)

Surface cracks around burst opening formed during ballooning at outer surface of cladding

Karlsruhe Institute of Technology

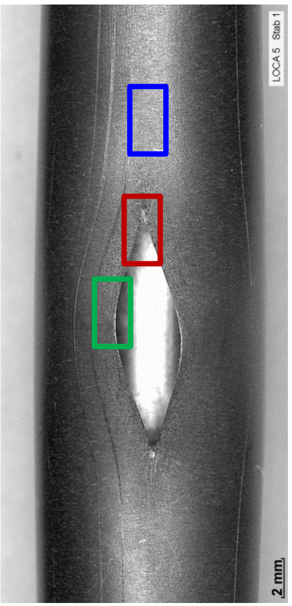

QL-5, rod #1

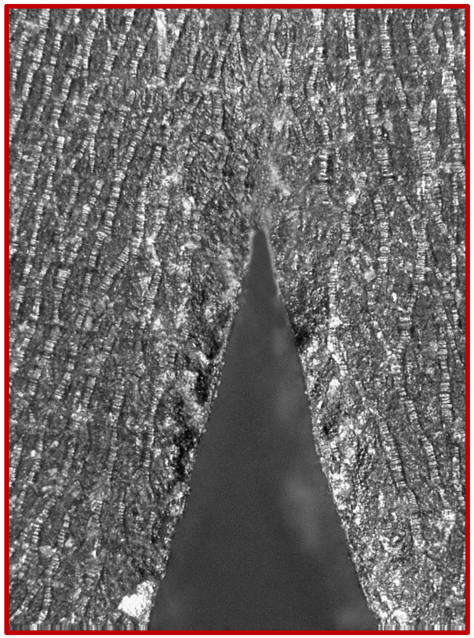

burst opening top, ≈ 20 cracks/mm

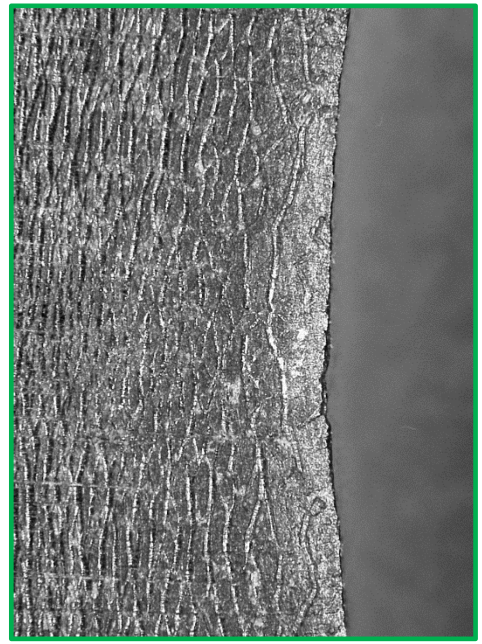

burst opening side, ≈ 20 cracks/mm

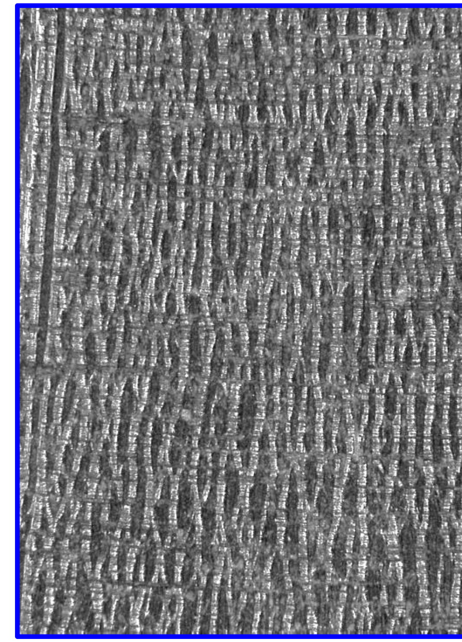

4 mm above opening tip, ≈ 40 cracks/mm

Videoscope observation of contact between pellet and cladding at inner cladding surface below burst opening

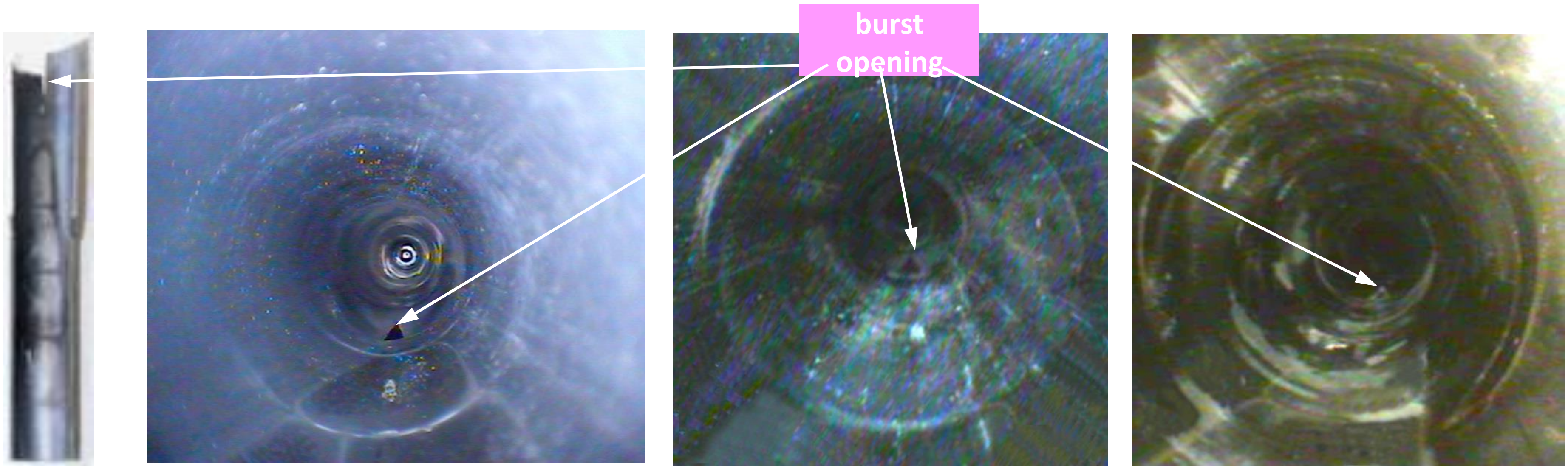

QL2, clad #8 | **QL4, endoscopy of rod #1** | **QL3, endoscopy of rod #5** | **QL5, endoscopy of rod #3**

Burst time and burst temperature

Test	average burst time, inner rods, s	average burst time, outer rods, s	average burst temperature, inner rods, K	average burst temperature, outer rods, K
QL-0 (Zry-4, 2.6 K/s)	124 ± 10	159 ± 9	1176 ± 26	1170 ± 31
QL-1 (Zry-4, 7 K/s)	58 ± 2	75 ± 7	1128 ± 31	1131 ± 30
QL-2 (M5®, 8 K/s)	52 ± 2	65 ± 3	*1148 ± 22*	1133 ± 27
QL-3 (ZIRLO, 8 K/s)	52 ± 2	63 ± 4	*1116 ± 13*	1118 ± 39
QL-3HT (ZIRLO, 7.5 K/s)	54 ± 3	70 ± 7	1127 ± 42	1127 ± 54
QL-4 (hydr. M5®, 8 K/s)	51 ± 3	62 ± 4	***1108 ± 13***	1106 ± 32
QL-5 (hydr. ZIRLO, 8 K/s)	54 ± 2	68 ± 4	***1065 ± 19***	1093 ± 42

Burst temperature of hydrogenated cladding is about 40 … 50 K lower in comparison to fresh cladding

Average geometrical parameters of burst openings

Test	max burst width, mm	burst length, mm	burst area, mm^2
QL0 (Zry-4, 2.6 K/s), bended rods	n. a.	12.7 ± 3.3	33.5 ± 21.1
QL1 (Zry-4, 7 K/s), strong bended rods	3.9 ± 2.6	14.5 ± 6.7	44.7 ± 49.2
QL2 (M5®, 8 K/s), bended rods	3.1 ± 1.2	13.5 ± 4.0	29.0 ± 22.9
QL3 (ZIRLO, 8 K/s)	3.9 ± 0.9	14.4 ± 2.2	31.0 ± 11.8
QL3HT (ZIRLO, 7.5 K/s), strong bended rods	n. a.	19.3 ± 7.3	n. a.
QL4 (hydr. M5®, 8 K/s)	3.3 ± 0.7	13.1 ± 2.0	24.1 ± 7.4
QL5 (hydr. ZIRLO, 8 K/s)	3.8 ± 0.6	14.3 ± 1.8	29.9 ± 8.8

Results of laser profilometry: typical axial distributions of the circumferential strain of claddings

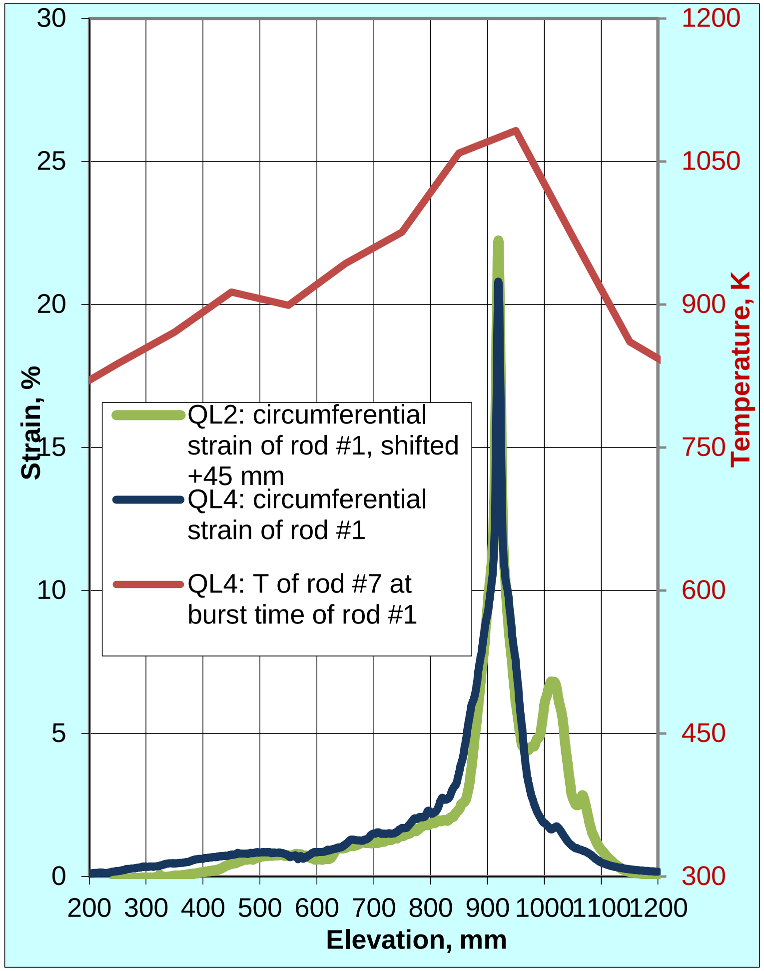

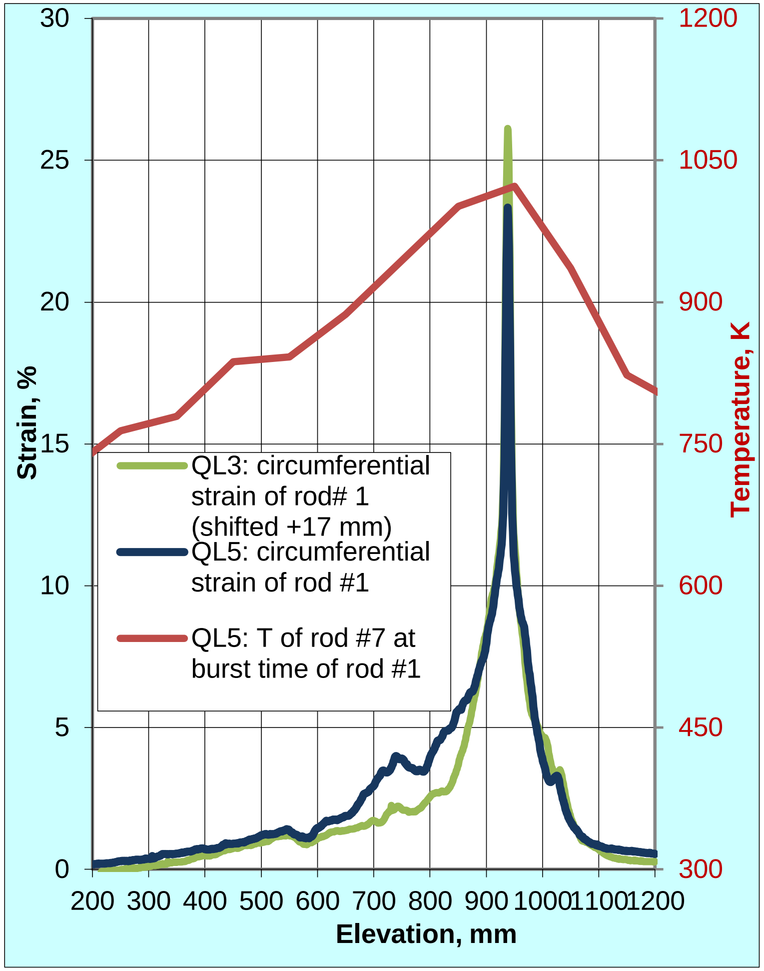

- additional ballooning peaks (alongside the main burst peak) formed during heat-up
- circumferential strain values in ballooning regions outside of burst opening are noticeably higher for the pre-hydrogenated claddings: cladding starts to creep earlier due to α→β transformation around dissolving hydrides

Results of laser profilometry: axial distribution of coolant channel blockages

Karlsruhe Institute of Technology

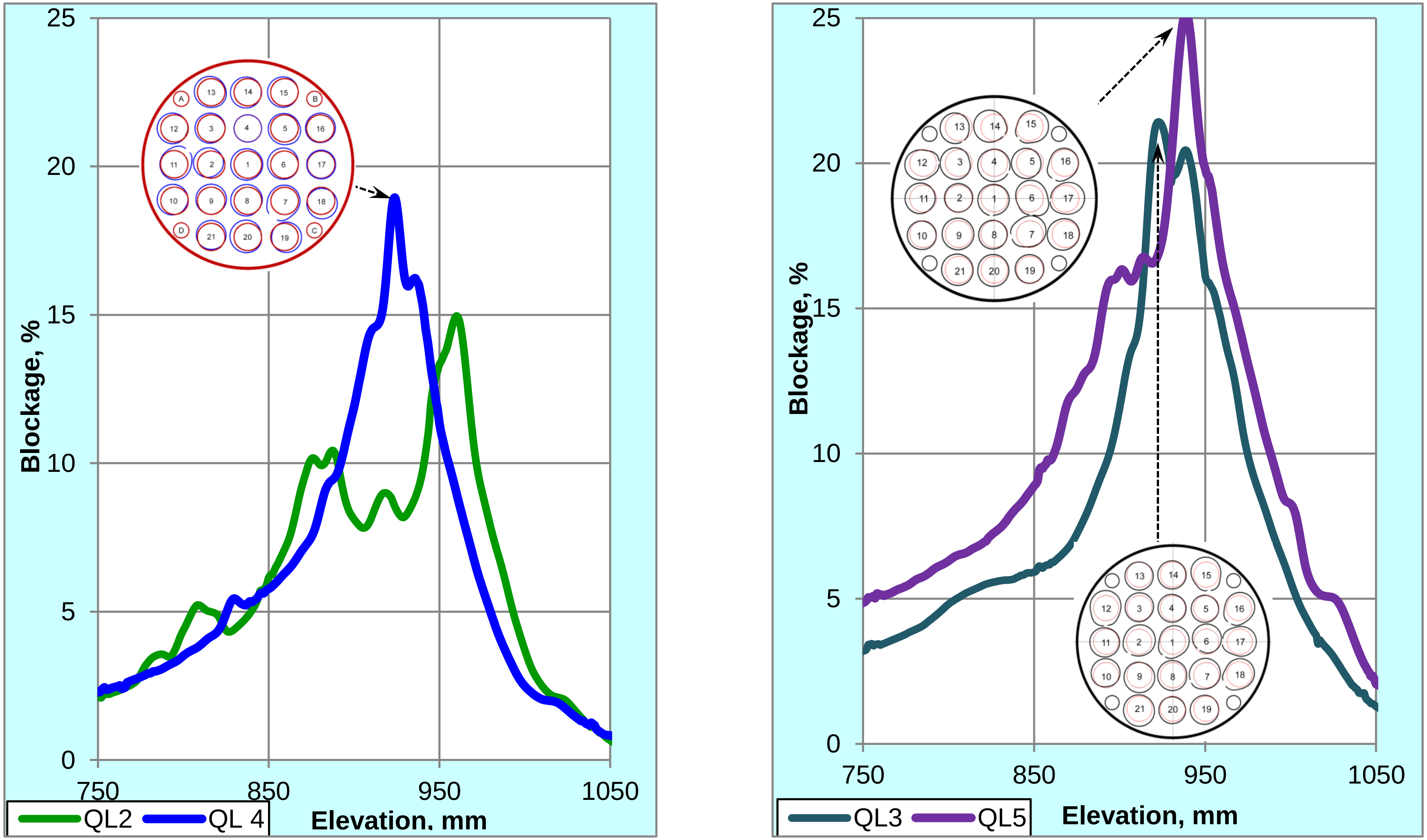

Ultrasound measurements: typical cladding wall thinning below and above the burst opening (rod #1, QUENCH-L5)

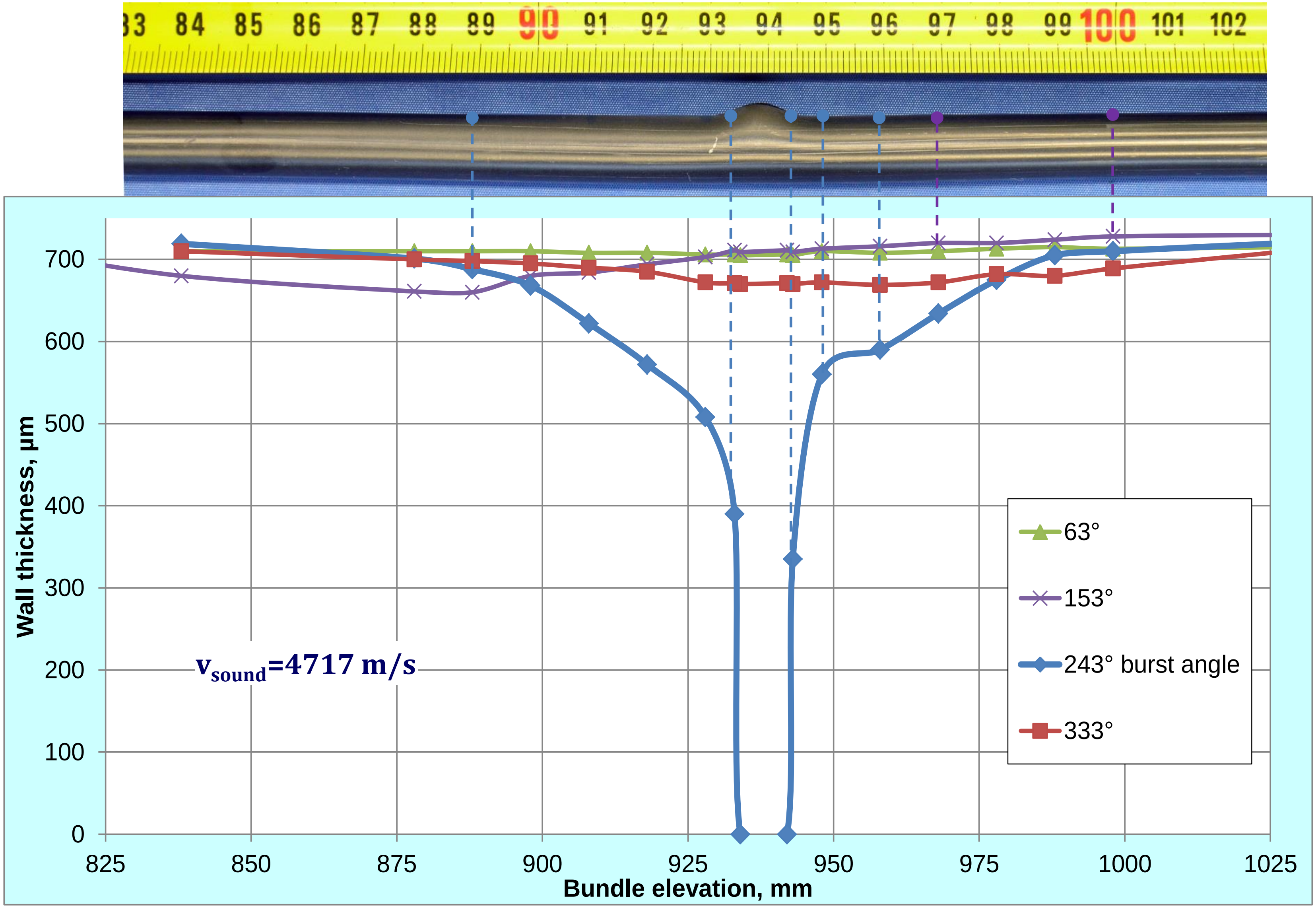

Eddy current measurements: axial distribution of oxidation rate (ZrO_2+α-Zr(O) outer layers)

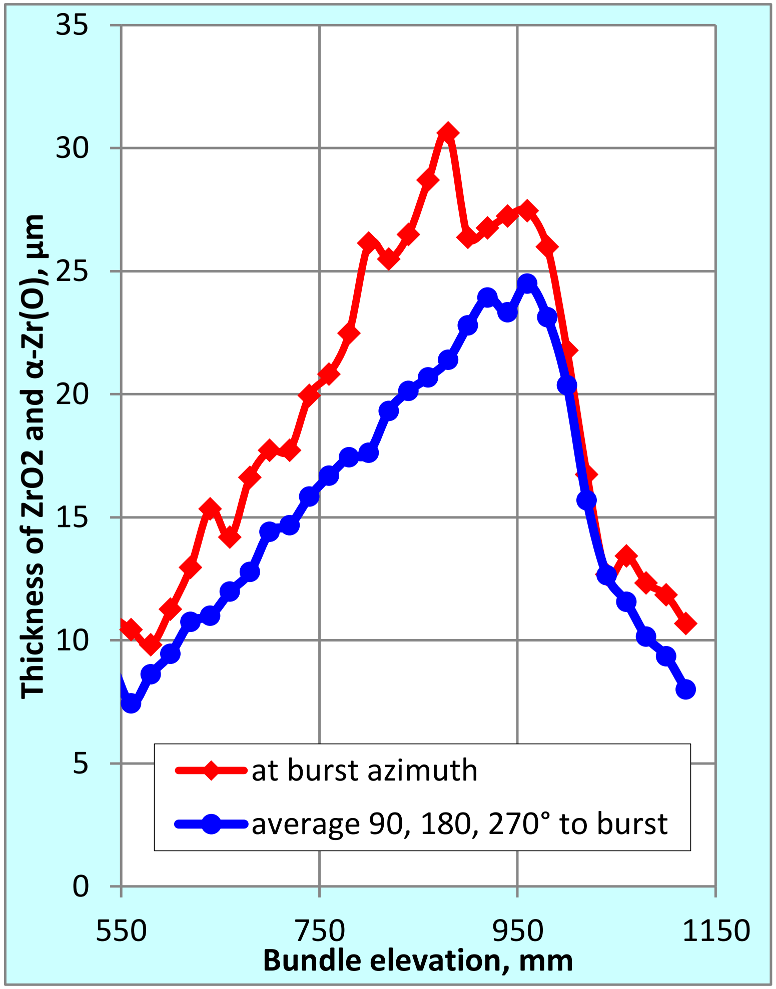

QL-4, central rod

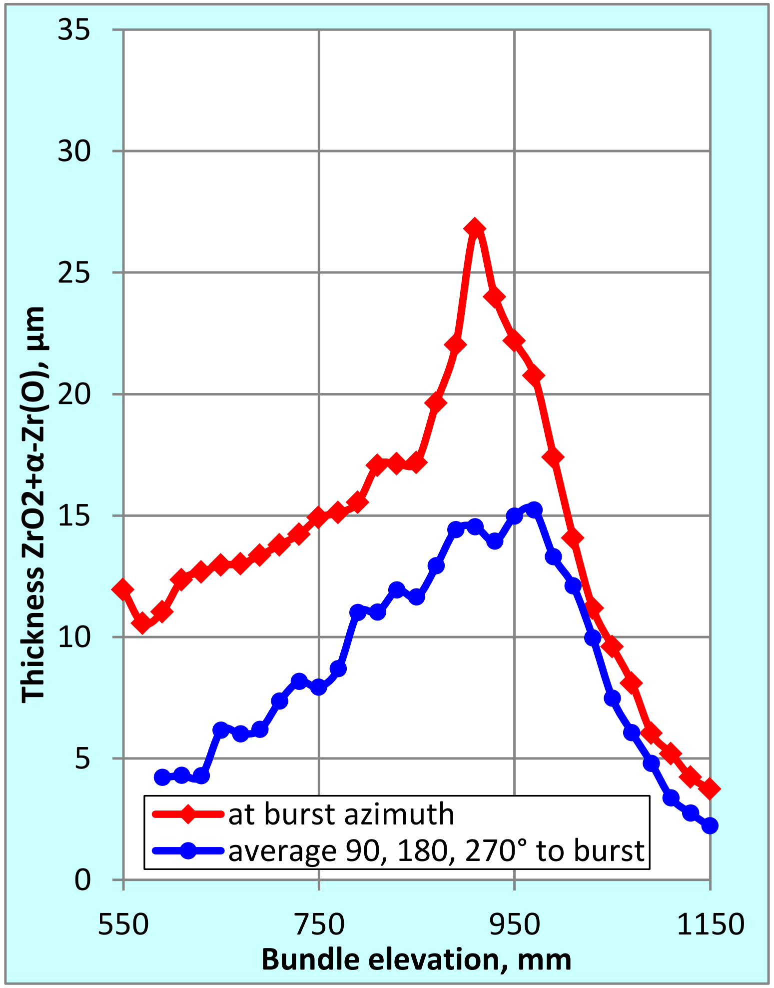

QL-5, central rod

Secondary hydrogenation of cladding

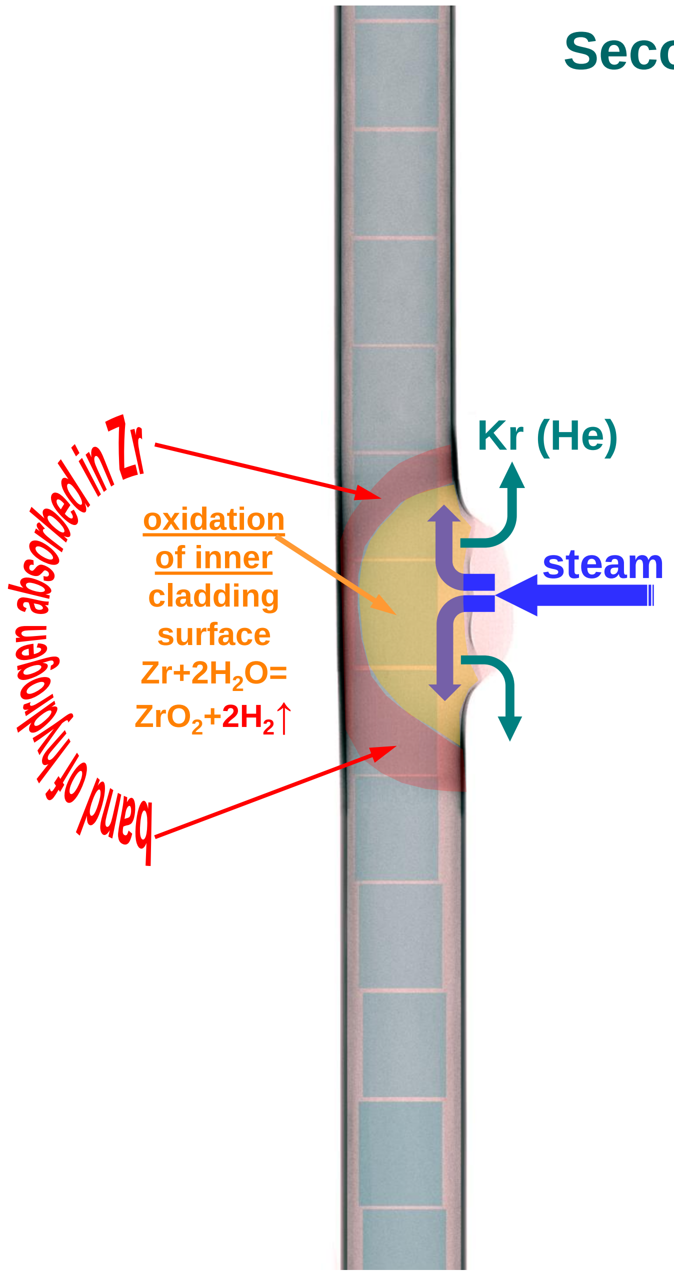

Sequence of phenomena during LOCA:

- cladding ballooning and burst, relief of inner rod pressure
- steam penetration through the burst opening, steam propagation inside the gap between cladding and pellet
- oxidation of inner cladding surface with hydrogen release
- absorption of hydrogen by cladding at the boundary of inner oxidised area at temperatures above the phase transition $\alpha \rightarrow (\alpha+\beta)$ in Zr alloy
- local embrittlement of cladding near to burst opening

Structures of inner cladding surface: thinning of inner oxide layer

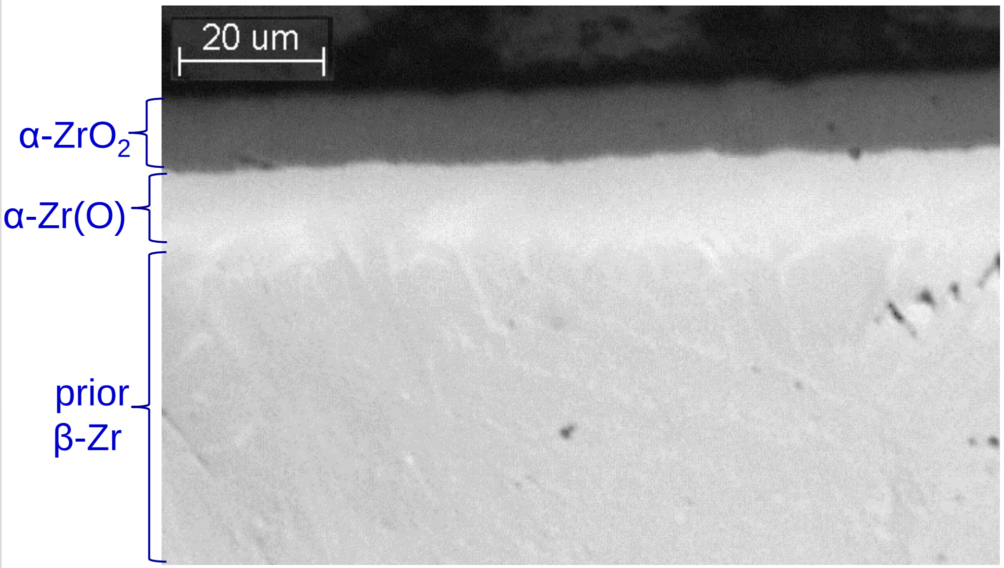

QL-4, clad #1: inner oxidation of cladding at the burst elevation

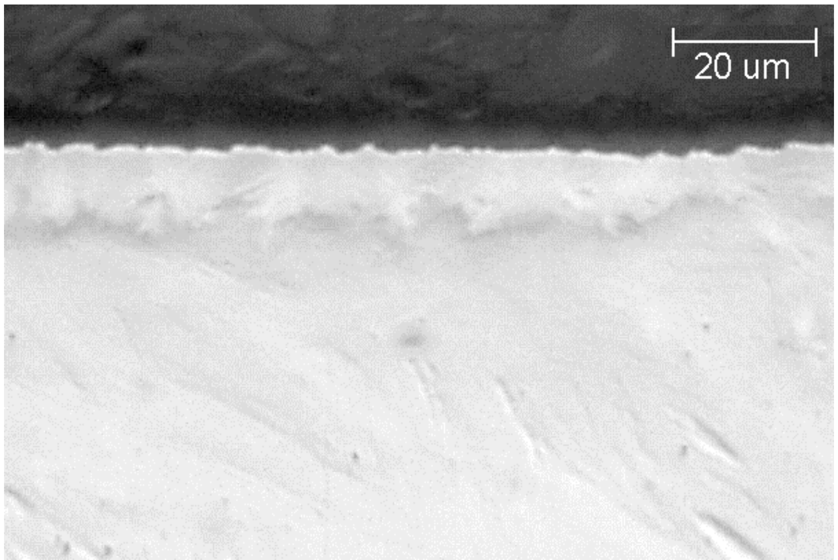

QL-4, clad #1: decreased inner oxidation of cladding at the elevation of hydrogen band

Neutron tomography: reconstruction of hydrogen distribution and determination of hydrogen concentration

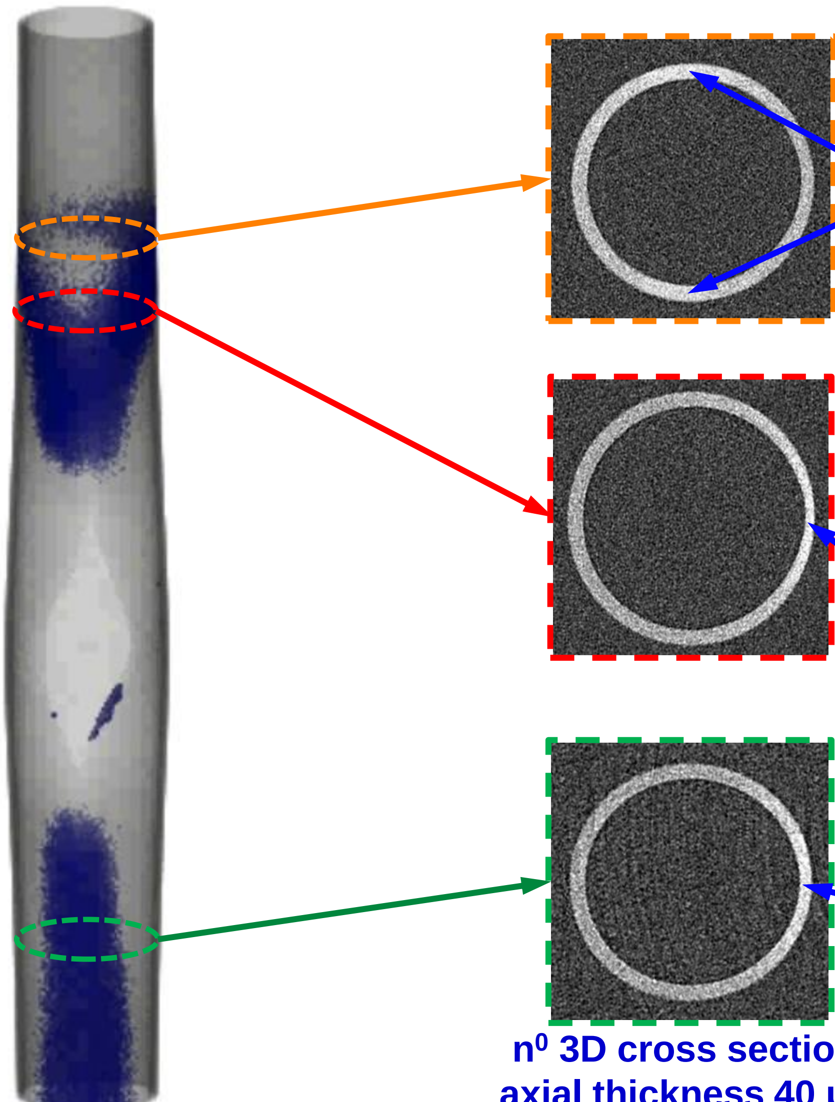

light spots max C_H

mean C_H = 475 ± 5 wppm,
local max C_H = 1430 ± 70 wppm

mean C_H = 278 ± 15 wppm,
local max C_H = 1450 ± 100 wppm

QL-3, clad #6, n^0 3D image

n^0 3D cross section, axial thickness 40 µm (voxel size)

Neutron tomography: axial distribution of hydrogen (mean and max values for each elevation)

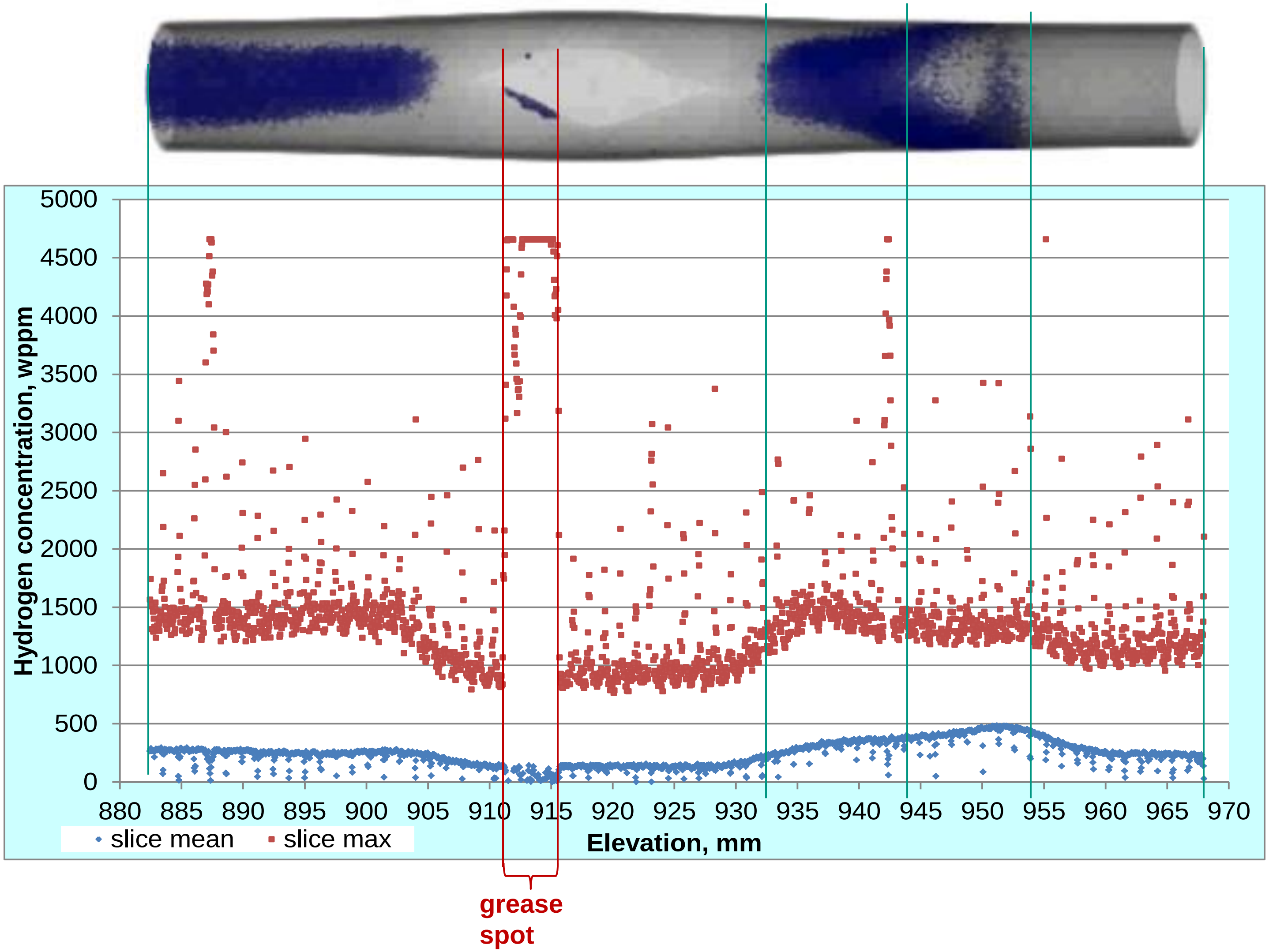

Axial maxima of the mean value of the hydrogen concentration (wppm) (results of n^0 tomography)

rod #	QL-0	QL-1	QL-2	QL-3	QL-3HT	QL-4 (H 100)	QL-5 (H 300)
1	1393		120			640	390
2		715	235	240			
3	845		240	180	2000	165	345
4				505	1940		
5				366			238
6			220	475		273	
7			170	363			327
8			440	307			
9			220	190		371	285
10				165		236	
11							
12			90				
13			150		940		
14			215			230	
16							
17							
18			150				
19							
20			160				
21			90				293

EBSD analysis of cladding region inside hydrogen band
(QL-4, central rod)

δ- and γ-hydrides

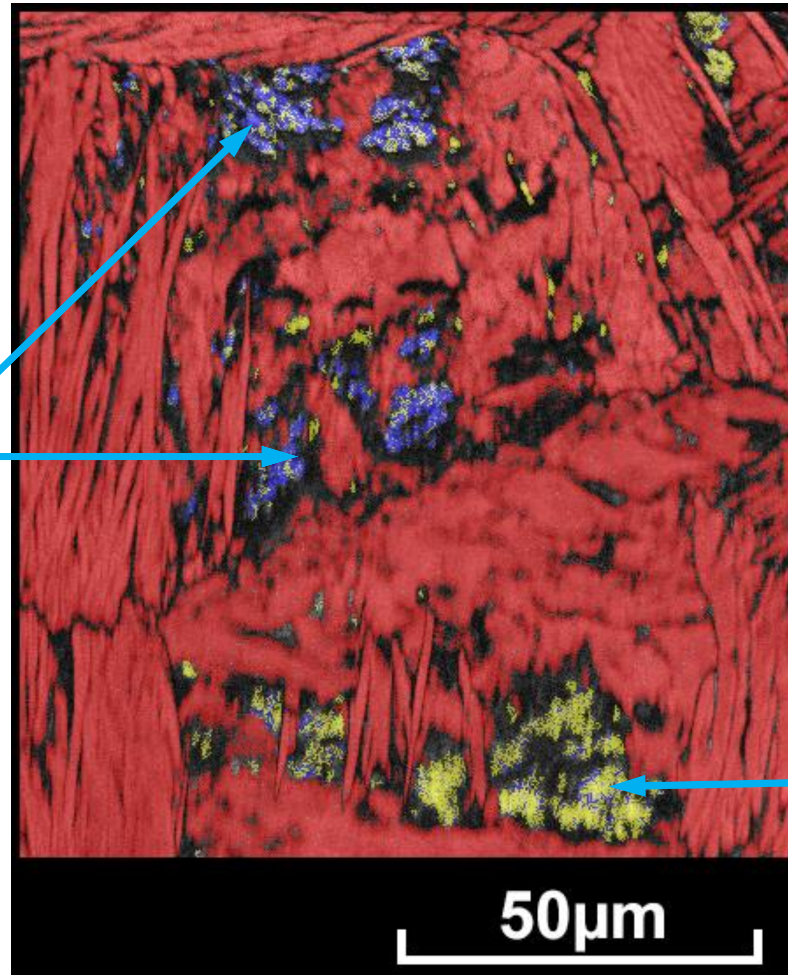

$\delta\text{-}ZrH_{1.66}$

hydride clusters near to boundaries of the region of coalesced grains with the same spatial orientation

Tensile test results: typical cladding fracture types

QL-4, clad #1
hydrogen embrittlement

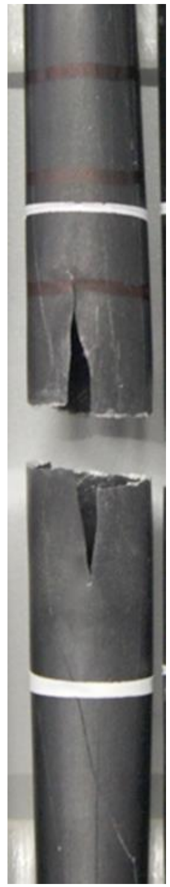

QL-3, clad #6

QL-3, clad #21

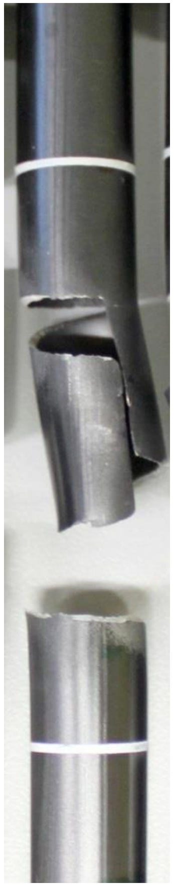

QL-4, clad #12

stress concentration at the edges of burst opening

QL-3, clad #12
necking far away from burst region

Tensile test results: typical parameters

Para-meter	QL-2		QL-4 100 wppm H		QL3		QL5 300 wppm H	
	stress conc.	necking	**stress conc.**	necking	**stress conc.**	necking	**stress conc.**	necking
ultimate tensile strength, MPa	**496**	507	**512**	520	**514**	521	**542**	554
fracture stress, MPa	**453**	384	**511**	402	**501**	385	**541**	448
elon-gation at fracture, %	**7.8**	11.2	**6.1**	9.7	**9.2**	11.0	**5.5**	9.0

Summary and conclusions

- Seven QUENCH-LOCA bundle tests with different cladding materials (Zry-4, M5®, Opt. ZIRLO™) were performed according to a temperature/time-scenario typical for a LBLOCA in a German PWR. For two tests (QUENCH-L4 and -L5) pre-hydrogenated claddings (with 100 and 300 wppm H for M5® and Opt. ZIRLO™, correspondingly) were used.
- Generally, a peak cladding temperature of about 1350 K (1250 K for QUENCH-L5) was reached at the end of the heat-up phase at the bundle elevation of 950 mm. The maximal heat-up rate was 8 K/s (2.6 K/s for commissioning test QUENCH-L0); the cooling phase lasted about 120 s (0 s for QUENCH-L0) and was terminated by 3.3 g/s/effective rod water flooding. The tangential temperature gradient across a rod was between 30 and 70 K on the burst onset (important parameter for ballooning size, accordingly to the REBEKA criterion).
- The detailed profilometry of the whole length of the rods showed formation of not only main ballooning area (with burst) but also, for several rods of each bundle, additional two or three ballooning regions. The reason should be the relatively long duration of the ballooning process at the main position and reaching of ballooning conditions (T>1000 K) at other bundle elevations.
- The maximal coolant channel blockage was less than 35% even for conservatively assuming coplanar ballooning. Due to this only moderate blockage, good bundle coolability was kept for all bundles.

Summary and conclusions (cont.)

- Cladding wall thinning from 725 to 350 µm due to ballooning was observed at the burst side along 50 mm below and above burst opening. The maximal oxide thickness at the outer cladding surfaces was less than 15 µm. Surface cracks, penetrating both layers, were formed in vicinity of burst opening during ballooning.
- Oxide layer formed after the burst at the inner cladding surface around the burst opening with a thickness of about 15 µm decreasing to 3 µm at a distance of about 20 mm from the burst opening.
- Hydrogen enrichments of a quite complex 3D form were observed for inner rods having seen peak cladding temperatures of more than 1200 K.
- Neutron tomography analysis showed the maximal hydrogen concentrations inside the hydrogen bands less of 750 wppm (averaged through the cladding cross section).
- EBSD analysis showed that a part of the hydrogen absorbed inside the claddings formed the hydrides with µm-sizes, which are distributed in the matrix intra as well inter granular. Another part of the absorbed hydrogen was probably dissolved in the metallic matrix.
- During quenching, following the high-temperature test stages, no fragmentation of claddings was observed (residual strengths and ductility were sufficient).
- Tensile tests at room temperature evidenced fracture at hydrogen bands for several inner rods with local hydrogen concentrations about 1500 wppm and more. Claddings with lower hydrogen concentrations fractured due to stress concentration at burst opening edges. Other tensile tested claddings failed after necking far away from burst region.

Acknowledgment

The QUENCH-LOCA experiments are supported and partly sponsored by the association of the German utilities (VGB). The M5® claddings and Zircaloy-4 spacer material were provided by AREVA. The opt. ZIRLO™ claddings and spacer material were provided by WESTINGHOUSE.

The authors would like to thank Mr. C. Rössger, Mr. J. Moch, Mrs. J. Laier and Mrs. U. Peters for intensive work during test preparation and post-test investigations, Dr. A. Pshenichnikov for the EBSD analysis, Dr. H. Leiste for the X-ray diffractometry measurements.

Thank you for your attention

https://www.iam.kit.edu/wpt/loca/
http://www.iam.kit.edu/awp/666.php
http://quench.forschung.kit.edu/